# The Structure of $B_8H_8^{2-}$ in Solution. Is $B_8H_9^-$ also Involved? An ab Initio/IGLO/NMR Study

**Michael Bühl,† Alexander Moiseevich Mebel,‡ Oleg Petrovich Charkin,‡ and Paul von Ragué Schleyer*,†**

Institut für Organische Chemie der Universität Erlangen-Nürnberg, Henkestrasse 42, D-8520 Erlangen, Germany, and Institute of New Chemical Problems, Russian Academy of Sciences, Chernogolovka, Moscow Region 142432, Russia

*Received October 7, 1991*

Ab initio calculations at the MP2/6-31G*//MP2/6-31G* + ZPE(6-31G*) level give relative energies of 0.0, 5.0, and 17.2 kcal/mol for the $D_{2d}$, $C_{2v}$, and $D_{4d}$ forms of $B_8H_8^{2-}$, respectively. Solvation (modeled by self consistent reaction field [SCRF] calculations) and ion pairing (computed for the $Li_2B_8H_8$ isomers) do not significantly affect the energetic relationships. The $C_{2v}$ form is a transient species involved in the fluxional rearrangement of the $D_{2d}$ form. The chemical shift calculations (IGLO) indicate that the fluxional $D_{2d}$ structure corresponds to the species which shows a single $\delta(^{11}B)$ NMR signal in solution. While no $B_8H_8^{2-}$ form was found to correspond with the 2:4:2 NMR chemical shift pattern, we raise the possibility that the second species observed under certain conditions might be the protonated form, $B_8H_9^-$ (**4**), rather than a second $B_8H_8^{2-}$ isomer. The observed $^{11}B$ NMR chemical shifts, the 2:4:2 intensity pattern, and the topomerization barrier (ca. 12 kcal/mol) all are consistent with the computed values for **4**.

## Introduction

Structural nonrigidity of polyhedral boranes and carboranes continues to be an explored intensively.[1-3] Of the basic *closo*-borane $B_nH_n^{2-}$ dianions, only $B_8H_8^{2-}$ (**1**)[4,5] and $B_{11}H_{11}^{2-}$,[6] show fluxional mobility at ambient temperatures. $B_8H_8^{2-}$ (**1**) is especially interesting since the structure found in the solid state appears not to predominate in solution.

The X-ray structure of **1** (as tetramino zinc salt) discloses a slightly distorted dodecahedron.[7] An idealized $D_{2d}$ geometry contains two sets of nonequivalent boron atoms. However, in polar solvents, **1** exhibits only one signal in the $^{11}B$ NMR spectrum (e.g. $\delta = -6.8$ ppm for $Cs_2B_8H_8$ in water).[4a] In less polar solvents, three peaks in a 2:4:2 ratio have been found (e.g. $\delta = -22.2, -3.6$, and 9.5 ppm for the $NBu_4^+$ salt in $CH_2Cl_2$/toluene at 4 °C).[4a] These collapse to the single signal at higher temperatures. Under special circumstances (e.g. $Na_2B_8H_8 \cdot xH_2O$ in $MeOCH_2CH_2OMe$), both the single and the 2:4:2 sets of signals are present at the same time. A barrier of ca. 12 kcal/mol was deduced. Muetterties, Hawthorne, et al. interpreted these results in terms of three polytopal isomeric forms which may interconvert, but not rapidly, on the NMR time scale.[4]

The single signal was assigned to the square antiprismatic form ($D_{4d}$ symmetry), whereas the 2:4:2 set was identified with the bicapped trigonal prism ($C_{2v}$, see Figure 1). The stability of $B_8H_8^{2-}$ forms was postulated to decrease with the number of square open faces; i.e., $D_{2d} > C_{2v} > D_{4d}$. However, Muetterties, Hawthorne et al. suggested that the interaction with counterions or with a polar solvent might stabilize species with square faces, and this might result in another stability order. A fluxional $D_{2d}$ form, which also could account for the single signal, was excluded: the boron scrambling mechanism should proceed via the $D_{4d}$ intermediate, but this was supposed to be in fast equilibrium with the $C_{2v}$ isomer. Hence, fluxional $D_{2d}$ and static $C_{2v}$ forms should not coexist.[4] We now report evidence refuting these interpretations: a fluxional $D_{2d}$ structure is present in solution.

In a subsequent theoretical paper,[5] Kleier and Lipscomb (KL) addressed the main aspects of the fluxional behavior of **1**. PRDDO calculations indicated the $D_{4d}$ form to be too high in energy (relative energy ca. 37 kcal/mol) to be present in significant amounts. The $D_{2d}$ form was computed to be the most stable isomer, but the $C_{2v}$ structure was only ca. 3 kcal/mol higher in energy. The interactions of **1** with $Li^+$ cations and with a HF molecule (as a solvent model) were found to have little influence on the relative energies of the various isomers.

Our objective was to reexamine and refine this study at modern computational levels. Additional information on the nature of the solution species is provided by IGLO chemical shift calculations.[9] The combined ab initio/IGLO/NMR method has been applied extensively to the elucidation of boron hydride structures.[10]

† Universität Erlangen-Nürnberg.
‡ Russian Academy of Sciences.

(1) (a) Wales, D. J.; Stone, A. J. *Inorg. Chem.* **1987**, *26*, 3845. (b) Wales, D. J.; Mingos, D. M. P.; Zhenyang, L. *Inorg. Chem.* **1989**, *28*, 2754. (c) Mingos, M. P.; Wales, D. J. In *Electron Deficient Boron and Carbon Clusters*; Olah, G. A., Wade, K., Williams, R. E., Eds.; Wiley: New York, 1991; Chapter 5, p 143.
(2) (a) Ott, J. J.; Brown, C. A.; Gimarc, B. M. *Inorg. Chem.* **1989**, *28*, 4269. (b) Gimarc, B. M.; Daj, B.; Warren, D. S.; Ott, J. J. *J. Am. Chem. Soc.* **1990**, *112*, 2597.
(3) (a) Gaines, D. F.; Coons, D. E.; Heppert, J. A. In *Advances in Boron and the Boranes*; Liebmann, F. F., Greenberg, A., Williams, R. E., Eds.; VCH Publishers: Weinheim, Germany, New York, 1988; Chapter 5, p 91. (b) Edvenson, G. M.; Gaines, D. F. *Inorg. Chem.* **1990**, *29*, 1210.
(4) (a) Muetterties, E. L.; Wiersema, R. J.; Hawthorne, M. F. *J. Am. Chem. Soc.* **1973**, *95*, 7520. (b) Muetterties, E. L. *Tetrahedron* **1974**, *30*, 1595. (c) Muetterties, E. L.; Hoel, E. L.; Salentine, C. G.; Hawthorne, M. F. *Inorg. Chem.* **1975**, *14*, 950.
(5) Kleier, D. A.; Lipscomb, W. N. *Inorg. Chem.* **1979**, *18*, 1312.
(6) (a) Tolpin, E. I.; Lipscomb, W. N. *J. Am. Chem. Soc.* **1973**, *95*, 2384. (b) Kleier, D. A.; Dixon, D. A.; Lipscomb, W. N. *Inorg. Chem.* **1978**, *17*, 166.
(7) Guggenberger, L. J. *Inorg. Chem.* **1969**, *8*, 2771.
(8) Independently, J. W. Bausch, G. K. S. Prakash, and R. E. Williams have reached the same conclusions regarding the $B_8H_8^{2-}$ structural question as reported at the BUSA-II Meeting, Research Triangle, NC, June 1990; see also: Williams, R. E. In *Electron Deficient Boron and Carbon Clusters*; Olah, G. A., Wade, K., Williams, R. E., Eds., Wiley: New York, 1990; Chapter 2, p 11 and footnotes 83b,c. Bausch, J. W.; Prakash, G. K. S.; Williams, R. E. *Inorg. Chem.*, preceeding paper in this issue.
(9) (a) Kutzelnigg, W. *Isr. J. Chem.* **1980**, *19*, 193. (b) Schindler, M.; Kutzelnigg, W. *J. Chem. Phys.* **1982**, *76*, 1919. (c) Review: Kutzelnigg, W.; Fleischer, U.; Schindler, M. *NMR, Basic Principles and Progress*, Springer Verlag: Berlin, 1990; p 165.
(10) (a) Schleyer, P. v. R.; Bühl, M.; Fleischer, U.; Koch, W. *Inorg. Chem.* **1990**, *29*, 153. (b) Bühl, M.; Schleyer, P. v. R. *Angew. Chem., Int. Ed. Engl.* **1990**, *29*, 886. (c) Bühl, M.; Schleyer, P. v. R. In *Electron Deficient Boron and Carbon Clusters*; Olah, G. A., Wade, K., Williams, R. E., Eds.; Wiley: New York, 1990; Chapter 4, p 113. (d) Bühl, M.; Schleyer, P. v. R.; McKee, M. L. *Heteroat. Chem.* **1991**, *2*, 499. (e) Bühl, M.; Schleyer, P. v. R. *J. Am. Chem. Soc.* **1992**, *114*, 477.

0020-1669/92/1331-3769$03.00/0 

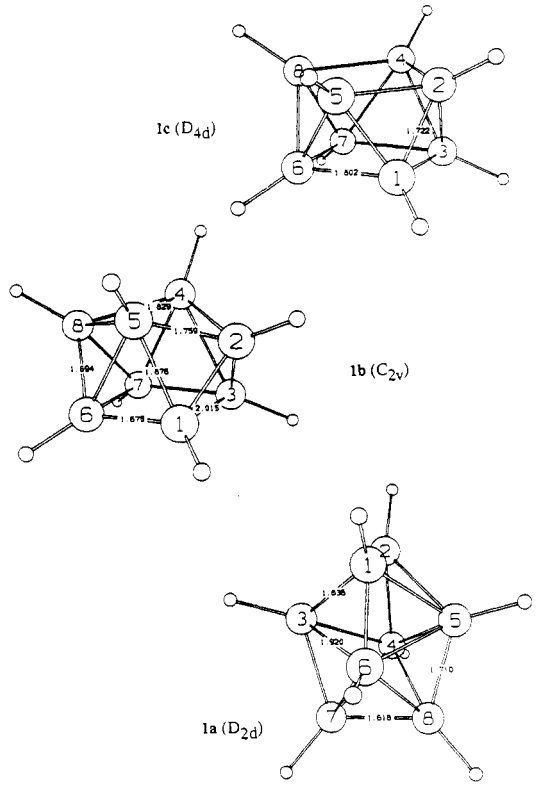


**Figure 1.** 6-31G* optimized geometries for $B_8H_8^{2-}$ **1a–1c**.

Since the structure of $B_8H_8^{2-}$ in solution has not been clarified, it seemed a particularly suitable candidate for a similar application.

$B_8H_9^-$ (**4**) i.e. protonated **1**, has not yet been synthesized, but has been examined computationally employing a STO-3G basis set and MNDO-optimized geometries.[11] The additional proton was predicted to be located over an edge at the "polar region" of a distorted dodecahedron. $B_8H_9^-$ represents another example of the protonated *closo*-borane dianions $B_nH_{n+1}^-$, which have been studied in detail both theoretically and experimentally.[12] The IGLO results for **4** indicated that it might be identified with the $B_8H_8^{2-}$ species that gives rise to the 2:4:2 NMR pattern (assigned to the $C_{2v}$ form of **1**). Hence, we decided to present the computational results for **1** and **4** together.

## Methods

The geometries were fully optimized in the given symmetry employing standrd procedures[13] and standard 3-21G and 6-31G* basis sets.[14] The Gaussian 90[15] and CADPAC[16] packages were used. Electron correlation effects were included in terms of Møller–Plesset perturbation theory to second order.[17] All orbitals were used for correlation throughout (Full MP2), notation MP2(FU)/6-31G*//6-31G*. In addition, the stationary points of **1** and the minima of **4** were optimized at that level (notation MP2(FU)/6-31G*//MP2(FU)/6-31G*). Of the possible isomeric forms of **3a–3c** only the more stable forms deduced from the PRDDO calculations[5] were considered. The nature of the stationary points was probed by frequency calculations at the 6-31G* level. None, one, and two imaginary frequencies denote minima, transition structures, and higher order stationary points, respectively.

**Table I.** Optimized Geometric Parameters for **1a–1c** (for Numbering Scheme see Figure 1) with Bond Distances in Å

| compd | level | B1B2 | B1B3 | B1B5 | B1B6 | B2B5 | B4B5 |
|---|---|---|---|---|---|---|---|
| **1a** | 6-31G* | 1.618 | 1.836 | | 1.710 | | 1.920 |
| | MP2/6-31G* | 1.611 | 1.806 | | 1.710 | | 1.889 |
| | expt[a] | 1.56 | 1.76 | | 1.72 | | 1.93 |
| **1b** | 6-31G* | 1.694 | 2.015 | 1.876 | 1.675 | 1.759 | 1.829 |
| | MP2/6-31G* | 1.676 | 1.947 | 1.821 | 1.681 | 1.752 | 1.847 |
| **1c** | 6-311G* | 1.722 | 1.802 | | | | |
| | MP2/6-31G* | 1.711 | 1.783 | | | | |

[a] Reference 8.

Solvation effects were studied by means of self-consistent reaction field (SCRF) calculations.[18] This modern adaption to the ab initio framework of the Onsager–Kirkwood–Westheimer cavity model, as implemented by Tomasi and his group,[19] provides a means for modeling continuum effects.

Chemical shifts were calculated using the IGLO (Individual Gauge for Localized Orbitals) method.[9] Huzinaga[20] basis sets were used which were contracted as follows: basis DZ, B 7s3p [4111,21], Li 7s [4111], H 3s [21]; basis II', B 9s5d1d [51111,2111,1], p-exponent 0.5 (H same as DZ).

## The Dianion $B_8H_8^{2-}$

**Relative Energies.** The HF/6-31G* structures of the $D_{2d}$ (**1a**), $C_{2v}$ (**1b**), and $D_{4d}$ (**1c**) forms are shown in Figure 1. Reoptimization at the MP2(FU)/6-31G* level resulted in minor changes in the geometric parameters (Table I). It is known from PRDDO calculations that other possible isomers are much higher in energy (>70 kcal/mol).[5] Hence, no other forms were considered.

Frequency analyses at HF/6-31G* established both **1a** and **1b** to be true minima on the potential energy surface (PES). In contrast, **1c** possesses two (degenerate) imaginary frequencies (343*i* $cm^{-1}$) denoting a second-order saddle point. Analysis of the normal mode vector shows that **1c** is a transition structure connecting two equivalent $D_{2d}$ forms. The 6-31G* IR frequencies show the strongest absorptions in the region around 2500 $cm^{-1}$. The number and the frequencies of the experimental IR bands

(11) Mebel, A. M.; Charkin, O. P.; Solntsev, K. A.; Kuznetsov, N. T. *Russ. J. Inorg. Chem. (Engl. Transl.)* **1989**, *34*, 156.
(12) See e.g.: (a) Privalov, V. I.; Tarasov, V. P.; Meladze, M. A.; Vinitskii, D. M.; Solntsev, K. A.; Buslaev, Y. A.; Kuznetsov, N. T. *Russ. J. Inorg. Chem. (Engl. Transl.)* **1986**, *31*, 5. (b) Mebel, A. M.; Charkin, O. P.; Solntsev, K. A.; Kuznetsov, N. T. *Russ. J. Inorg. Chem. (Engl. Transl.)* **1989**, *34*, 808; **1989**, *34*, 813. (c) Mebel, A. M.; Charkin, O. P.; Solntsev, K. A.; Kuznetsov, N. T. *Russ. J. Inorg. Chem. (Engl. Transl.)* **1988**, *33*, 1292. For reviews see: (d) Kuznetsov, N. T.; Solntsev, K. A. In *Chemistry of Inorganic Hydrides*; Kuznetsov, N. T., Ed.; Nauka, Publ.: Moscow, **1990**, (in Russian); p 5. (e) Mebel, A. M.; Charkin, O. P. In *Chemistry of Inorganic Hydrides*; Kuznetsov, N. T., Ed.; Nauka Publ.: Moscow, 1990, (in Russian); p 43.
(13) Hehre, W.; Radom, L.; Schleyer, P. v. R.; Pople, J. A. *Ab Initio Molecular Orbital Theory*; Wiley: New York, 1986.
(14) (a) 3-21G: Binkley, J. S.; Pople, J. A.; Hehre, W. J. *J. Am. Chem. Soc.* **1980**, *102*, 939. (b) Gordon, M. S.; Binkley, J. A.; Pople, J. A.; Petro, W. J.; Hehre, W. J. *J. Am. Chem. Soc.* **1982**, *104*, 2797. (c) 6-31G*: Hariharan, P. C.; Pople, J. A. *Theor. Chim. Acta*, **1973**, *28*, 213. (d) Francl, M. M.; Pietro, W. J.; Hehre, W. J.; Binkley, J. S.; Gordon, M. S.; DeFrees, D. J.; Pople, J. A. *J. Chem. Phys.* **1982**, *77*, 3654.
(15) Frisch, M. J.; Head-Gordon, M.; Trucks, G. W.; Foresman, J. B.; Schlegel, H. B.; Raghavachari, K.; Robb, M. A.; Binkley, J. S.; Gonzales, C.; DeFrees, D. J.; Fox, D. J.; Whiteside, R. A.; Seeger, R.; Melius, C. F.; Baker, J.; Martin, R. L.; Kahn, L. R.; Stewart, J. J. P.; Topiol, S.; Pople, J. A. *Gaussian 90*; Gaussian Inc.: Pittsburgh, PA, 1990.
(16) Amos, R. D.; Rice, J. E. *CADPAC: The Cambridge Analytical Derivatives Package*, Issue 4.0, Cambridge, 1987.
(17) Binkley, J. S.; Pople, J. A. *Int. J. Quantum. Chem.* **1975**, *9*, 229 and references therein.
(18) Tomasi's SCRF procedure using spherical cavities around the atoms was installed in the Convex version of Gaussian 82 (Binkley, J. S.; Whiteside, R. A.; Raghavachari, K.; Seeger, R.; DeFrees, D. J.; Schlegel, H. B.; Frisch, M. J.; Pople, J. A.; Kahn, L. *Gaussian 82*; Carnegie-Mellon University; Pittsburgh, PA, 1982). Note that in this version the SCRF calculations are performed at the SCF level. The sphere radii used for the atoms were 20% larger than the van der Waals radii. The solvent effect calculations employed the temperature (298.15 K), as well as the following physical constants: the solvent diameters, densities, thermal expansion coefficients, and the dielectric constants (taken from: Riddick, J. A.; Bunger, W. B.; Sahano, T. K. *Organic Solvents*; Wiley: New York, 1986; Vol. 2.)
(19) (a) Onsager, L. *J. Am. Chem. Soc.* **1936**, *58*, 1486. (b) Kirkwood, J. G.; Westheimer, F. H. *J. Chem. Phys.* **1938**, *6*, 506. (c) Miertus, S.; Scrocco, E.; Tomasi, J. *Chem. Phys.* **1981**, *55*, 117. (d) Pascal-Ahuir, J. L.; Tomasi, J.; Bonaccorsi, R. *J. Comput. Chem.* **1987**, *8*, 778. (e) Rivail, J. L.; Terryn, B.; Rinaldi, D.; Ruiz-Lopez, M. F. *THEOCHEM* **1985**, *120*, 387.
(20) Huzinaga, S. *Approximate Atomic Wave Functions*, University of Alberta: Edmonton, Canada, 1971.

**Table II.** Calculated IR Wavenumbers[a] and Intensities[b] (6-31G* Basis Set) for **1a–1c**

| expt[c] | 1a | [intens] | 1b | [intens] | 1c | [intens] |
|---|---|---|---|---|---|---|
| 2480 (vs) | 2540 | [1126] | 2576 | [143] | 2528 | [1405] |
| | | | 2540 | [1008] | | |
| 2450 (vs) | 2522 | [838] | 2524 | [760] | | |
| | | | 2521 | [118] | 2513 | [1080] |
| | 2497 | [406] | 2502 | [839] | | |
| | 2487 | [58] | 2486 | [536] | | |
| | | | 2478 | [415] | | |
| 1138 (m) | 1222 | [50] | 1190 | [34] | 1168 | [40] |
| | | | 1140 | [6] | | |
| 1000 (vw) | 1093 | [15] | 1124 | [37] | | |
| 950 (vw) | 1009 | [4] | 1047 | [10] | | |
| | | | 1014 | [2] | | |
| | | | 977 | [1] | | |
| 900 (w) | 950 | [8] | 963 | [8] | | |
| | | | 960 | [2] | | |
| | | | 947 | [2] | | |
| 860 (w) | 877 | [4] | 894 | [33] | 899 | [3] |
| 834 (vw) | | | 857 | [2] | | |
| | | | 848 | [4] | | |
| | | | 816 | [5] | | |
| | | | 811 | [1] | | |
| 715 (vw) | 692 | [3] | 763 | [12] | 777 | [12] |
| | | | 735 | [5] | | |
| 660 (vw) | 640 | [5] | 669 | [1] | 617 | [2] |
| 630 (w) | 607 | [5] | 657 | [4] | | |
| 620 (w) | | | 591 | [1] | | |
| | | | 527 | [1] | | |

[a] Harmonic frequencies, $cm^{-1}$. [b] kM/mol. [c] $Rb_2B_8H_8$, Nujol mull, ref 19, assignment tentative.

(for $Rb_2B_8H_8$, determined in Nujol)[21] are probably best reconciled with the $D_{2d}$ form **1a** (see data in Table II).

The relative energies of **1a–1c** in Table III show only modest changes with the theoretical level. The PRDDO results are in good accord with the 6-31G* values. Inclusion of electron correlation and zero point corrections [MP2(FU)/6-31G*//MP2-(FU)/6-31G* + ZPE(6-31G*) level] slightly disfavors **1b** and stabilizes **1c**, resulting in our final relative energies (vs **1a**) of ca. 5 and 17 kcal/mol, respectively. Hence, the free dianion shows a strong preference for the $D_{2d}$ form.

**Solvation and Ion Pairing.** Mutterties suggested that a polar solvent might stabilize structures with square faces and result in the predominance of the $D_{4d}$ form in solution.[4] However, KL have shown that the interaction energies of **1a** and **1b** with a single HF molecule (serving as a solvent model) are relatively small (binding energies < 5 kcal/mol)[5] and are not specific. We were interested in the bulk medium effect of a polarizable continuum as assessed by SCRF calculations.[18,19] In special cases, solvation effects based on such a continuum model have been shown to influence molecular properties significantly.[22]

We performed single point calculations for the MP2 geometries of **1a–1c**, employing the 6-31G* basis set and the physical constants for water. The overall effect of solvation on the relative energies is indicated to be quite small (compare the 6-31G*//6-31G* and SCRF($H_2O$)/6-31G* results in Table III). In fact, the SCRF calculations reveal a small destabilization of **1b** and **1c** with respect to the isolated dianions. Hence, no preferential stabilization of structures with square faces due to solvation is apparent.

Ion pairing is another factor that might favor species with square faces.[4] This possibility also was addressed by KL who calculated various $LiB_8H_8^-$ (**2**) and $Li_2B_8H_8$ (**3**) isomers, but only in partially optimized structures (e.g. the $B_8H_8^{2-}$ units were

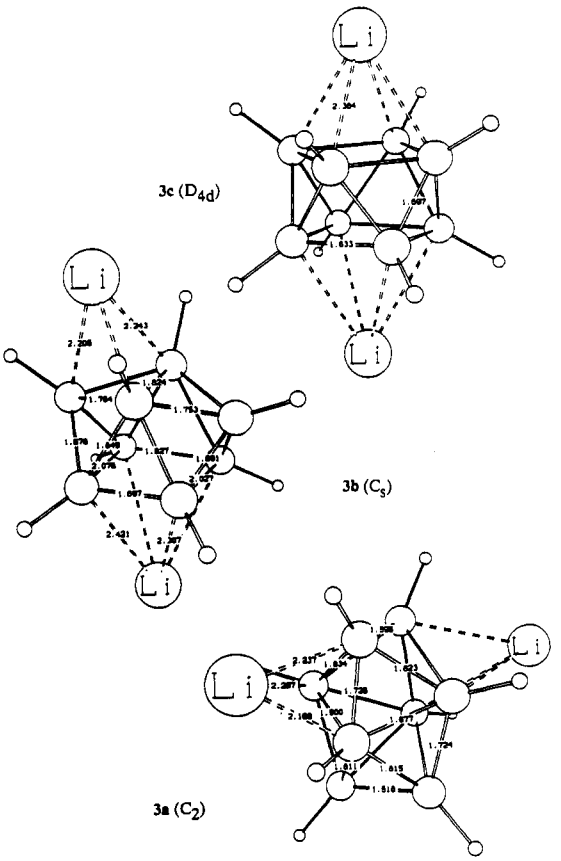


**Figure 2.** 6-31G* optimized geometries for $Li_2B_8H_8$ **3a–3c**.

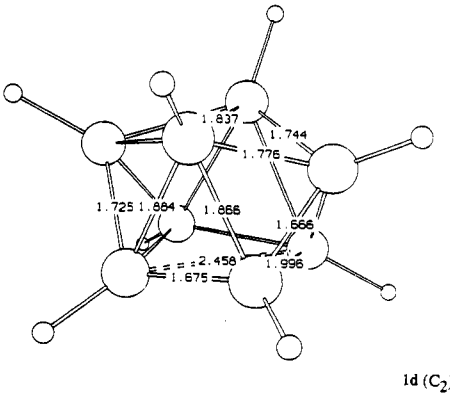


**Figure 3.** Transition state **1d** between **1a** and **1b**, 6-31G* optimized.

frozen).[5] While KL found that attachment of one $Li^+$ indeed stabilizes the $C_{2v}$ form with respect to the $D_{2d}$ isomer by ca. 2 kcal/mol, addition of the second $Li^+$ reestablishes the energetic sequence of the naked dianions.

We performed complete geometry optimizations for the ion pairs of **1a** and **1b** with one and two lithium cations. The relative energies of the doubly lithiated compounds **3a**, **3b**, and **3c** (Figure 2) are 0.0, 5.5, and 19.9 kcal/mol, respectively (MP2/6-31G*//6-31G* + ZPE level, Table III). These are nearly identical to the relative energies of the free dianions **1a–1c**, in accord with the results of KL.[5]

Like **1c**, **3c** is not a minimum on the PES. Moreover, **3c** has four imaginary frequencies! In addition to the vibrations describing the distortion of the boron cage, there are two very small degenerate vibrations ($12i$ $cm^{-1}$) corresponding to the displacement of the lithium cations from the centers of the square faces.

In contrast to KL,[5] we do not find an energetic reversal of **1a** and **1b** upon attachment of a single $Li^+$: the ion pair derived from the $C_{2v}$ dianion (**2b**, $Li^+$ attached to the square face) is 5.5 kcal/

(21) Klanberg, F.; Eaton, D. R.; Guggenberger, L. J.; Muetterties, E. L. *Inorg. Chem.* **1967**, *6*, 1271.

(22) See e.g.: (a) Steinke, T.; Hänsele, E.; Clark, T. *J. Am. Chem. Soc.* **1989**, *111*, 9107. (b) Bühl, M.; Steinke, T.; Schleyer, P. v. R.; Boese, R. *Angew. Chem.*, **1991**, *103*, 1179. (c) Wong, M. W.; Frisch, M. J.; Wiberg, K. B. *J. Am. Chem. Soc.* **1991**, *113*, 4776.

**Table III.** Absolute (au) and Relative Energies (kcal/mol, in Brackets) for **1–3**

| level of theory | **1a**, $D_{2d}$ | **1b**, $C_{2v}$ | **1c**, $D_{4d}$ |
|---|---|---|---|
| ZPE(6-31G*)[a] | 68.1 (0) | 68.1 (0) | 67.4 (2) |
| 6-31G*//6-31G* | 202.00006 [0.0] | 201.99548 [2.9] | 201.96155 [24.2] |
| MP2/6-31G*//6-31G* | 202.80187 [0.0] | 202.79296 [5.6] | 202.77434 [17.3] |
| MP2/6-31G*[b] | 202.80345 [0.0] | 202.79556 [5.0] | 202.77510 [17.8] |
| final[c] | [0.0] | [5.0] | [17.2] |
| SCRF($H_2O$)/6-31G* | 202.64254 [0.0] | 202.63371 [5.5] | 202.59939 [27.1] |

| level of theory | **2a**, $C_s$ | **2b**, $C_{2v}$ |
|---|---|---|
| ZPE(6-31G*) | 70.3 (0) | 70.2 (0) |
| 6-31G*//6-31G* | 209.59700 [0.0] | 209.58952 [4.7] |
| MP2/6-31G*//6-31G* | 210.41334 [0.0] | 210.40452 [5.5] |

| level of theory | **3a**, $C_2$ | **3b**, $C_s$ | **4c**, $D_{4d}$ |
|---|---|---|---|
| ZPE(6-31G*) | 71.9 (0) | 71.8 (0) | 69.9 (4) |
| 6-31G*//6-31G* | 217.04676 [0.0] | 217.04305 [2.3] | 217.00459 [26.5] |
| MP2/6-31G*//6-31G* | 217.87511 [0.0] | 217.86613 [5.6] | 217.84334 [19.9] |

[a] 6-31G* zero point energy. In parentheses: number of imaginary frequencies. [b] MP1/6-31G*//MP2/6-31G*. [c] MP2/6-31G*//MP2/6-31G* + ZPE(6-31G* level; the zero point energies have been scaled by 0.89 as recommended in ref 11.

**Table IV.** IGLO $^{11}$B Chemical Shifts of **1–3** (in ppm)

| | **1a** (4:4) | | | **1b** (2:4:2) | | | |
|---|---|---|---|---|---|---|---|
| level of theory | 4 | 4 | ($\phi$)[a] | 2 | 4 | 2 | **1c** |
| DZ//6-31G* | −2.1 | −10.6 | (−6.4) | −14.3 | 11.0 | 8.3 | 5.6 |
| DZ//MP2/6-31G* | −2.5 | −13.4 | (−8.0) | −15.7 | 7.0 | 7.9 | 4.4 |
| II'//MP2/6-31G* | −1.0 | −14.6 | (−7.8) | −16.4 | 6.2 | 9.5 | 3.5 |
| expt[b] | | | −6.8 | −22.2 | −3.6 | 9.5 | |

| | | **2b** (2:4:2) | | |
|---|---|---|---|---|
| level of theory | **2a** | 2 | 4 | 2 |
| DZ//6-31G* | (−3.4)[a] | −4.0 | 14.1 | 32.3 |

| | | **3b**[a] | | | |
|---|---|---|---|---|---|
| level of theory | **3a** | 2 | 4 | 2 | **3c** |
| DZ//6-31G* | (−6.4)[a] | −10.2 | 14.4 | 21.6 | 14.2 |

[a] Averaged values. [b] Reference 4a.

mol higher in energy than the ion pair derived from the $D_{2d}$ form (**2a**, $Li^+$ attached to the B1B2B3 face). Like solvation, ion pairing effects apparently do not stabilize **1b** or **1c**, preferentially.

**Transition State between $D_{2d}$ and $C_{2v}$.** In studies of polyhedral rearrangements, several authors noted that the transformation of **1a** to **1b** in $C_2$ symmetry is an "allowed process".[1a,5] Only minor changes of orbital and total energies along a linear synchronous transit pathway were found, and a very small activation barrier was anticipated.

We optimized the transition state **1d** ($C_2$ symmetry, Figure 3) connecting the two minima **1a** and **1b**. The nature of this stationary point was verified by frequency analysis (one imaginary frequency). If one starts from **1b**, **1d** is an early transition state: the B···B distances of the bond being formed in this process are 2.620, 2.458, and 1.920 Å for **1b**, **1d**, and **1a**, respectively, at the 6-31G* level. At this level, the barrier indeed is very small (less than 0.1 kcal/mol). Inclusion of electron correlation and zero point correction (MP2/6-31G*//6-31G* + ZPE) even stabilizes **1d** with respect to **1b** (−0.5 kcal/mol). Hence, isolated **1b** is not a stable species, but is expected to rearrange spontaneously to **1a** without any barrier.

However, as suggested by KL, **1b** is very likely to be an intermediate (or perhaps a transition state on the $\Delta H$ or $\Delta G$ hypersurface) involved in the boron scrambling of **1a**. Cleavage of the B(3)B(6) bond in **1a** followed by closure of the B(1)B(7) diagonal in the transient species **1b** permutes two pairs of the nonequivalent boron nuclei. This affords a good example of the well-known diamond–square–diamond (DSD)[23] rearrangement.

(23) Lipscomb, W. N. *Science* **1966**, *153*, 373.

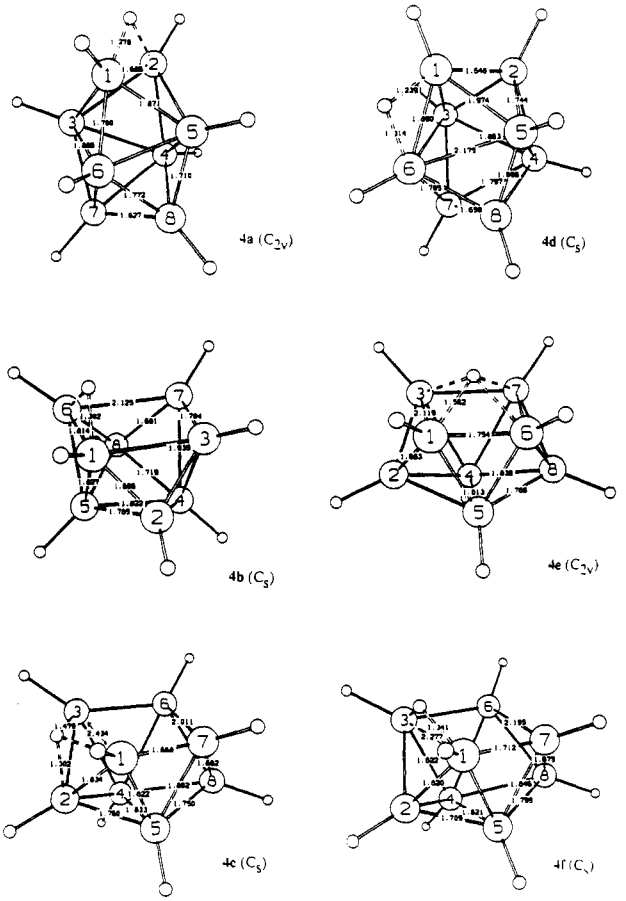


**Figure 4.** 6-31G* optimized geometries for $B_8H_9^-$ **4a–4f**.

A rapid sequence of such processes would therefore account for the single $^{11}$B signal observed in the NMR spectra.

**Chemical Shift Calculations.** The IGLO chemical shifts for **1–3** are summarized in Table IV. The IGLO $^{11}$B value for the $D_{4d}$ form **1c**, the proposed structure identified with the single boron resonance observed in solution,[4] is +3.5 ppm (II'//MP2/6-31G*). This result deviates by more than 10 ppm from the experimental value, −6.8 ppm.[4a] The usual accuracy of the chemical shifts calculated at that level is ca. 2 ppm for neutral and anionic boron hydrides.[10c] Hence, we consider structure **1c** to be quite unlikely, based on the IGLO result. Ion pairing is predicted to cause a downfield shift (even further away from experiment): IGLO $\delta(^{11}B)$ = 14.2 ppm for **3c**.

The IGLO chemical shifts for the static $D_{2d}$ form **1a** are −1.0

**Table V.** Absolute (au) and Relative (kcal/mol, in Brackets) Energies for Different Structures of the $B_8H_9^-$ Ion

| level of theory | **4a**, $C_{2v}$ | **4a'**, $C_s$ | **4b**, $C_s$ | **4c**, $C_s$ |
|---|---|---|---|---|
| ZPE(3-21G)[a] | 76.4 (1) | 76.9 (0) | 76.5 (0) | 75.8 (0) |
| 3-21G//3-21G | 201.52519 [4.3] | 201.52594 [3.8] | 201.53200 [0] | 201.51642 [9.8] |
| 6-31G*//6-31G* | 202.68658 [0.03] | 202.68662 [0] | 202.68559 [0.6] | 202.67079 [9.9] |
| MP2/6-31G*//6-31G*[b] | 203.44734 [0] | 203.44695 [0.2] | 203.43148 [10.0] | 203.41643 [19.0] |
| MP2/6-31G*[c] | 203.49535 [0] | | 203.48009 [9.6] | |
| final[d] | [0 (0)] | [0.6] | [10.1(9.7)] | [18.5] |

| level of theory | **4d**, $C_s$ | **4e**, $C_{2v}$ | **4f**, $C_s$ |
|---|---|---|---|
| ZPE(3-21G) | 76.1 (1) | 74.0 (1) | 74.3 (1) |
| 3-21G//3-21G | 201.51594 [10.1] | 201.52361 [5.3] | 201.49795 [21.4] |
| 6-31G*//6-31G* | 202.67207 [9.1] | 202.67437 [7.7] | 201.64914 [23.5] |
| MP2/6-31G*//6-31G* | 203.42562 [13.1] | 203.42667 [13.0] | 203.39374 [33.6] |
| final[d] | [12.8] | [10.9] | [31.7] |

[a] 3-21G zero point energy. In parentheses: number of imaginary frequencies. [b] MP2(frozen core)/6-31G*//6-31G* energy. [c] MP2(full)/6-31G*//MP2(full)/6-31G* energy. [d] MP2(FC)/6-31G*//6-31G*+ZPE(3-21G). In parentheses: MP2(FU)/6-31G*//MP2(FU)/6-31G*+ZPE(3-21G); ZPE's scaled by 0.89 as recommended in ref 11.

and −14.6 ppm (Table IV). However, fluxionality is expected. This leads to an averaged IGLO $\delta(^{11}B)$ of −7.8 ppm, which agrees well with the measured value of −6.8 ppm.[4a] Ion pairing is indicated to have little influence on the mean value of the chemical shifts: **2a** (with one $Li^+$) shows a small downfield shift (to −3.4 ppm), whereas the averaged IGLO values of **1a** and **3a** (with two $Li^+$'s) are identical (−6.4 ppm, DZ//6-31G* values).

We cannot reconcile the observed 2:4:2 resonance pattern with the $C_{2v}$ form **1b**: the deviations of one of the IGLO values (−16.4, 6.2, and 9.5 ppm, Table IV) from the experimentally reported chemical shifts (−22.2, −3.6, and 9.5) is up to ca. 10 ppm. As for **1c**, ion pairing is predicted to cause substantial downfield shifts, which would result in worse agreement of calculated and experimental data (Table IV). The IGLO data underscore the conclusion that the $C_{2v}$ form **1b** does not exist (except perhaps as a transient species involved in scrambling of **1a**). The energetic results discussed above agree.

### The $B_8H_9^-$ Monoanion

**Geometry.** Our systematic survey of the $B_8H_9^-$ potential energy surface (PES) started from different configurations of the $B_8H_8^{2-}$ (**1a–1c**) dianion, with the additional proton occupying various coordination sites (triangular and tetragonal faces, edges, and vertices, respectively). As a result, a number of stationary points on the PES were located (Figure 4).

The most stable $B_8H_9^-$ structure is **4a** ($C_{2v}$ symmetry), with the extra hydrogen $H^1$ localized above the B1B2 edge (four-coordinated boron atoms in the $D_{2d}$ form $B_8H_8^{2-}$ **1a**). At SCF levels, **4a** possesses one imaginary frequency (−233*i* and −105*i* $cm^{-1}$ at 3-21G and 6-31G*, respectively) denoting a transition state. At those levels, the minimum energy structure **4a'** possesses $C_s$ symmetry with the bridge bond $BH^1B$ slightly bent toward the B1B2B5 face (for geometric parameters see Table VI). However, inclusion of electron correlation renders **4a** more stable than **4a'** by 0.2 kcal/mol (MP2(FC)/6-31G*//6-31G*, Table V). Moreover, the attempted geometry optimization of **4a'** in $C_s$ symmetry at the MP2(FU)/6-31G* level leads to the more symmetric **4a** ($C_{2v}$). Hence, the minimum is **4a** rather than **4a'**. Apparently the PES in this region is extremely flat. The boron skeleton in **4a** is distorted to some extent with respect to that of unprotonated **1a** by the influence of the extra hydrogen (Table VI). The bridged B1B2 bond is elongated by 0.04 Å (MP2/6-31G*). The adjacent B1B3 and B1B6 bond lengths increase by 0.03 and 0.06 Å, respectively. The "equatorial belt" of the cluster (i.e. the B3B4 bond) is somewhat contracted by ca. 0.02 Å. The B4B7 edge lengths decrease by 0.05 Å. Note that the skeletal deformation in $B_8H_9^-$ as compared with the $B_8H_8^{2-}$ dianion is essentially smaller than the deformation of $B_6H_7^-$ and $B_{10}H_{11}^-$ compared with $B_6H_6^{2-}$ and $B_{10}H_{10}^{2-}$, respectively.[12] Although, the terminal B1H and B2H bonds hardly vary in length, their bending away from the XB axis (X = the center of mass) is significant (up to 18–20°).

**Table VI.** Optimized Geometric Parameters for $B_8H_9^-$ with Bond Distances in Å (SCF/6-31G*; in parentheses; MP2/6-31G*).

| | **4a**, $C_{2v}$ | **4a'**, $C_s$ | **4b**, $C_s$ | **4c**, $C_s$ | **4d**, $C_s$ | **4e**, $C_{2v}$ | **4f**, $C_s$ |
|---|---|---|---|---|---|---|---|
| B1B2 | 1.686 (1.654) | 1.689 | 1.696 (1.682) | 1.834 | 1.648 | 1.683 | 1.820 |
| B1B3 | 1.871 (1.833) | 1.837 | 2.125 (2.025) | 2.434 | 1.974 | 2.119 | 2.277 |
| B2B3 | | | 1.681 (1.662) | | 1.744 | | |
| B1B5 | | 1.915 | 1.827 (1.814) | 1.822 | | 1.836 | 1.822 |
| B2B5 | | | 1.785 (1.761) | 1.760 | | 1.766 | 1.709 |
| B1B6 | 1.780 (1.770) | 1.775 | 1.814 (1.793) | 1.668 | 1.890 | 1.754 | 1.712 |
| B2B4 | | | 1.719 (1.715) | | 1.708 | | |
| B3B4 | 1.886 (1.867) | 1.909 | 1.935 (1.854) | | 1.863 | | |
| B4B5 | | 1.862 | 1.822 (1.833) | 1.833 | | 1.813 | 1.821 |
| B5B6 | | | | 1.862 | 2.175 | | 1.846 |
| B3B6 | | | 2.758 (2.674) | 2.771 | | 2.751 | 2.816 |
| B4B7 | 1.772 (1.752) | 1.777 | | | 1.797 | | |
| B4B8 | | 1.775 | | 1.750 | | | 1.795 |
| B6B7 | | | | 2.011 | 1.785 | | 2.195 |
| B6B8 | | | | 1.682 | | | 1.675 |
| B3B7 | 1.710 (1.703) | 1.698 | 1.704 (1.700) | | 1.696 | | |
| B7B8 | 1.627 (1.627) | 1.625 | | | 1.659 | | |
| $BH^1$ | 1.278 (1.295) | 1.279 | 1.302 (1.298) | 1.302 | 1.239 | 1.562 | 1.341 |
| | | | | 1.479 | 1.314 | | |

Besides the global minimum **4a**, two local $B_8H_9^-$ minima were found, **4b** and **4c**. In **4b**, the additional hydrogen is situated over the B1B6 edge of the $C_{2v}$ form **1b** of the reference $B_8H_8^{2-}$. At the highest level employed, MP2(FU)/6-31G*//MP2(FU)/6-31G*+ZPE(3-21G), **4b** is 9.7 kcal/mol higher in energy than **4a**. Hence, protonation increases the energy difference between the parent $D_{2d}$ and $C_{2v}$ forms of $B_8H_8^{2-}$ (5.0 kcal/mol). The elongation of some of the bonds of **1b** upon protonation to give **4b** are quite pronounced: e.g. 0.11 Å for the bridged B1B6, and 0.08 Å (MP2/6-31G*) for the adjacent B1B3 and B6B7 bonds.

The third $B_8H_9^-$ minimum (**4c**) is 18.5 kcal/mol less stable than **4a**. In **4c** the extra hydrogen is located over the B1B2B3 face of $B_8H_8^{2-}$ (**1b**), but opening of the boron skeleton results. The B1B3 separation increases to 2.43 Å; i.e., the bond is broken. The B1B2 and B2B3 bonds between the boron atoms interacting with $H^1$ are elongated by 0.14 Å, and the adjacent B1B5 and B3B4 bond lengths increase by 0.06 Å. The extra hydrogen in **4c** is situated over one side of a nonplanar pentagonal face.

**Nonrigid Behavior.** The transition state **4d** (with $H^1$ over the B1B6 edge **1a**) between isomers **4a** and **4b** involves $H^1$ transfer from B1B2 in **4a** to B1B6 in **4d**. The B3B6 bond increases in length (to 2.18 Å) in **4d**, and the bond breaks completely in going to **4b**. $H^1$ moves above the B1B6 edge of the planar tetragonal B1B6B7B3 face. Transition structure **4d** is 12.8 kcal/mol higher in energy than **4a**, but lies only 2.7 kcal/mol above **4b**. Hence, the local minimum **4b** is separated from the much more stable global minimum **4a** by a very small barrier. Similarly, the $C_{2v}$ form of $B_8H_8^{2-}$ was predicted to rearrange to **1a**, though without any barrier. The additional hydrogen in $B_8H_9^-$ destabilizes the structure with a tetragonal face and makes the boron skeleton

**Table VII.** Calculated IR Wavenumbers[a] and Intensities[b] (3-21G Basis Set) for $B_8H_9^-$

| **4a**, $C_{2v}$[c] | | **4a'**, $C_s$ | **4b**, $C_s$ | **4c**, $C_s$ | **4d**, $C_s$ | **4e**, $C_{2v}$ | **4f**, $C_s$ |
|---|---|---|---|---|---|---|---|
| 560 [7] | 588 [8] | 252 [9] | 341 [14] | 101 [4] | 302 [10] | 343 [5] | 224 [4] |
| 662 [7] | 674 [9] | 660 [7] | 539 [42] | 451 [8] | 684 [8] | 738 [6] | 433 [4] |
| 833 [11] | 820 [5] | 724 [5] | 597 [10] | 615 [37] | 714 [13] | 742 [25] | 501 [6] |
| 873 [5] | 885 [6] | 876 [7] | 762 [6] | 695 [14] | 801 [6] | 894 [15] | 660 [5] |
| 912 [8] | 937 [10] | 933 [8] | 788 [26] | 733 [62] | 814 [5] | 935 [29] | 737 [66] |
| 941 [11] | 965 [10] | 941 [10] | 799 [6] | 741 [6] | 840 [11] | 966 [7] | 777 [7] |
| 1053 [6] | 1048 [11] | 1012 [7] | 912 [15] | 789 [20] | 911 [7] | 1063 [43] | 814 [30] |
| 1155 [26] | 1184 [32] | 1163 [25] | 1002 [7] | 879 [12] | 986 [5] | 1439 [15] | 856 [34] |
| 1962 [1] | 2034 [0.4] | 1959 [10] | 1075 [5] | 989 [6] | 1087 [6] | | 878 [14] |
| 2145 [11] | 2145 [20] | 2146 [12] | 1113 [9] | 1095 [7] | 1151 [16] | | 926 [8] |
| | | | 1150 [18] | 1098 [11] | 1892 [13] | | 1101 [28] |
| | | | 1841 [122] | 1147 [7] | 2357 [33] | | 1136 [11] |
| | | | 1948 [27] | 1336 [40] | | | 1506 [24] |
| | | | | 1976 [25] | | | 1906 [490] |
| 2724 [24] | 2665 [34] | 2703 [157] | 2690 [92] | 2689 [139] | 2694 [135] | 2734 [64] | 2703 [96] |
| 2726 [137] | 2667 [286] | 2736 [55] | 2703 [335] | 2696 [239] | 2715 [21] | 2735 [110] | 2705 [122] |
| 2738 [18] | 2668 [22] | 2737 [133] | 2725 [22] | 2728 [113] | 2723 [79] | 2745 [409] | 2720 [378] |
| 2740 [378] | 2689 [393] | 2747 [442] | 2732 [164] | 2731 [119] | 2727 [133] | 2757 [443] | 2730 [6] |
| 2751 [497] | 2691 [36] | 2754 [412] | 2737 [191] | 2749 [436] | 2732 [207] | 2760 [460] | 2737 [302] |
| 2753 [341] | 2703 [647] | 2758 [170] | 2746 [364] | 2760 [286] | 2733 [496] | 2778 [14] | 2741 [405] |
| 2776 [18] | 2709 [436] | 2779 [43] | 2748 [344] | 2764 [34] | 2744 [333] | | 2752 [24] |
| | | | 2770 [85] | 2792 [154] | 2766 [99] | | 2801 [183] |

[a] Harmonic frequencies, $cm^{-1}$. [b] kM/mol. [c] Left column, 3-21G; right column, 6-31G*.

slightly more rigid toward the DSD rearrangement. In $B_8H_9^-$, this process is coupled with the migration of the extra hydrogen. Rapid **4a** $\rightarrow^{4d}$ **4b** $\rightarrow^{4d'}$ **4a*** rearrangements (rupture and closure of different bonds) would scramble all the boron atoms. Hence, our computed activation barrier for this process is 12.8 kcal/mol as compared with ~5.1 kcal/mol in $B_8H_8^{2-}$.

In isomer **4b**, degenerate migration of the extra hydrogens can occur from the B1B6 edge to the B3B7 edge via transition state **4e**; the barrier is only 0.8 kcal/mol. In **4e** ($C_{2v}$) the extra $H^1$ is situated over the center of the tetragonal B1B6B7B3 face and interacts with four boron atoms, resulting in a 0.10-Å elongation of the B1B3 and B6B7 edges as compared with **1b**.

The transition state between **4b** and **4c** is the form **4f** with the extra hydrogen over the longer edge (B1B3) of the tetragonal face of $B_8H_8^{2-}$ (**1b**) ($C_{2v}$). Structure **4f** lies 31.7 kcal/mol above the global minimum **4a**. Starting from **4c**, the barrier for the arrangement to **4b** is 13.2 kcal/mol. A scanning of the PES of **4c** shown that movement of the extra hydrogen toward the B1B2 edge results in a much stronger increase of energy than its migration to the B1B3 edge (toward **4f**). Thus, the lowest energy pathway of the transformation of **4c** to **4a** involves isomer **4b**: **4c** $\rightarrow^{4f}$ **4b** $\rightarrow^{4d}$ **4a**. Hence, **4c** is stabilized kinetically by a barrier of 13.2 kcal/mol, and might in principle be observed experimentally under special conditions.

The feasible rearrangements in $B_8H_9^-$ are summarized in the following scheme:

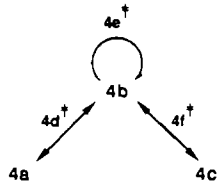


In contrast to the higher $B_nH_{n+1}^-$ homologues,[12] the configurations of $B_8H_9^-$ with terminal $BH_2$-groups are higher order saddle points (three and two imaginary frequencies, respectively), and are not competitive energetically (up to 50 kcal/mol less stable at the 3-21G level). Hence, these forms were not refined at higher levels.

**IR Frequencies.** Significant changes in vibrational spectra are computed for the various structures of $B_8H_9^-$ as compared with $B_8H_8^{2-}$. The data summarized in Table VII reveal a noticeable shift of the terminal BH bond stretch vibrations to higher wave numbers (150–190 $cm^{-1}$). Similar trends were found both experimentally and theoretically for $B_6H_7^-$ and $B_{10}H_{11}^-$.[12] Characteristic features of the IR spectra are associated with the bridging hydrogen.[24] These frequencies for the global minimum **4a** are 2030 and 2270 $cm^{-1}$ (SCF/6-31G*) and correspond to vibrations of the critical bridge bond (movement of the extra $H^1$ perpendicular to and parallel with the direction of the bridged BB edge, respectively). For the transition structure **4d**, the latter vibration is shifted to 2357 $cm^{-1}$). Lower frequencies characterize the vibrations of the bridge $BH^1B$ bonds in the structures with tetragonal faces: 1841 and 1948 $cm^{-1}$ (**4b**); 1336 and 1976 $cm^{-1}$ (**4c**); and 1506 and 1906 $cm^{-1}$ (**4f**) (SCF/3-21G).

**Chemical Shift Calculations.** The IGLO chemical shifts for the various structures of $B_8H_9^-$ are summarized in Table VIII. Four signals with equal intensity are expected in the $^{11}B$ NMR spectrum of the global minimum **4a**. However, the computed chemical shifts are very similar for B1, B2 (–0.9 ppm) and B4, B6 (–1.5 ppm) (II'/MP2/6-31G*). Hence, the spectrum might appear to consist of only three peaks with $\delta(^{11}B)$ = +12.9, –0.9 (–1.5), and –26.3 ppm, with an intensity ratio of 2:4:2. Interestingly, these IGLO prediction closely resemble the experimental $\delta(^{11}B)$ values reported for $B_8H_8^{2-}$ in nonpolar solvents (9.5, –3.6, and –22.2 ppm). The original assignment to a $C_{2v}$ form[4] is now doubtful on the basis of our ab initio and IGLO calculations. $B_8H_8^{2-}$ is basic enough to deprotonate water (or other proton donors) present in solution. The calculated proton affinity (PA) for $OH^-$ is 381.9 kcal/mol at the MP2(FU)/6-31+G*//MP2-(FU)6-31+G* + ZPE(6-31G*) level. The PA computed [MP2-(FC)/6-31+G*//MP2(FU)/6-31G* + ZPE(6-31G*)] for the $B_8H_8^{2-}$ dianion is much higher, 413.1 kcal/mol.[25] Thus, the reaction $B_8H_8^{2-} + H_2O \rightarrow B_8H_9^- + OH^-$ is exothermic in gas phase and, probably, in solution. Hence, significant amounts of $B_8H_9^-$ might be present. We suggest that **4a** might be the species giving rise to the 2:4:2 $^{11}B$ NMR pattern.

Furthermore, the barrier for the degenerated rearrangement **4a** $\rightarrow$ **4b** $\rightarrow$ **4a*** (12.8 kcal/mol), which scrambles all boron atoms,

(24) (a) Buzek, P.; Schleyer, P. v. R.; Sieber, S.; Koch, W.; Carneiro, J. W. de M.; Vancik, H.; Sunko, D. E. *J. Chem. Soc. Chem. Commun.* **1991**, 671. (b) Buzek, P.; Schleyer, P. v. R.; Vancik, H.; Sunko, D. E. *J. Chem. Soc. Chem. Commun.* **1991**, 1538.

(25) The computed PA value for $B_8H_8^{2-}$ is lower by 24 kcal/mol than that for $B_6H_6^{2-}$, but it is higher by 28 kcal/mol than that for $B_{10}H_{10}^{2-}$ (SCF/3-21G).[12e] Both $B_6H_7^-$ and $B_{10}H_{11}^-$ are found experimentally.[12a,d]

**Table VIII.** IGLO $^{11}B$ Chemical Shifts (ppm) for the $B_8H_9^-$ Anion

| | 4a | | | | 4b | | | | | | |
|---|---|---|---|---|---|---|---|---|---|---|---|
| level of theory | B(1,2) | B(4,6) | B(3,5) | B(7,8) | B(1,6) | B(3,7) | B(1,6,3,7)[a] | B(2,8) | B4 | B5 | B(4,5)[a] |
| DZ//6-31G* | +0.5 | +1.9 | −23.7 | +10.6 | +17.4 | +34.1 | (+25.8) | +32.7 | +18.9 | −18.8 | (+0.1) |
| DZ//MP2/6-31G* | +0.3 | +2.4 | −25.4 | +11.5 | +14.5 | +25.0 | (+19.8) | +38.4 | +12.7 | −18.6 | (−3.0) |
| II'//MP2/6-31G* | −1.5 | −0.9 | −26.3 | +12.9 | +12.9 | +25.2 | (+19.1) | +42.2 | +10.4 | −19.2 | (−4.4) |

| | 4a' | | | | | | | 4c | | | | |
|---|---|---|---|---|---|---|---|---|---|---|---|---|
| level of theory | B(1,2) | B(4,6) | B3 | B5 | B(3,5)[a] | B7 | B8 | B(7,8)[a] | B(1,3) | B2 | B(4,5) | B(6,7) | B8 |
| DZ//6-31G* | +0.04 | +1.0 | −22.9 | −22.5 | (−22.7) | +4.1 | +15.6 | (+9.9) | +23.7 | +1.2 | −11.3 | +8.6 | +30.3 |

| | 4d | | | | | | 4e | | |
|---|---|---|---|---|---|---|---|---|---|
| level of theory | B1 | B2 | B(3,5) | B4 | B6 | B(7,8) | B(1,3,6,7) | B(2,8) | B(4,5) |
| DZ//6-31G* | +4.0 | +19.4 | +5.3 | −10.5 | +8.4 | +10.9 | +8.8 | +5.8 | −7.6 |

[a] Averaged values.

agrees well with the experimental value, 12 kcal/mol, ascribed to $B_8H_8^{2-}$ (**1b**).[4] A remaining problem is that there would have to be a significant barrier for proton exchange between **1a** and **4a**, since both sets of signals are present under certain conditions. Also, the temperature dependence of the spectra would implicate the (reversible) gain and loss of a proton as a function of the temperature, which would probably be unprecedented in boron hydride chemistry. Clearly, further experimental investigations are desirable.

The averaged chemical shift computed for **4a**, −4.0 ppm (II'//MP2), differs only by 2.8 ppm from the experimental value for $B_8H_8^{2-}$, −6.8 ppm. This might complicate the experimental recognition of the protonated form. However, IR spectra should allow a reliable discrimination between $B_8H_9^-$ and $B_8H_8^{2-}$ (see above).

## Conclusion

Both the energetic and NMR criteria indicate the $D_{2d}$ form **1a** to be the most stable $B_8H_8^{2-}$ isomer and to be present in solution. Since **1a** is fluxional, it exhibits only one signal in the $^{11}B$ NMR spectrum. The $C_{2v}$ isomer **1b** is only a transient species involved in the scrambling process of **1a**. The $D_{4d}$ form **1c** does not exist at all.

Energetic evidence indicate that the additional hydrogen in $B_8H_9^-$ is situated above the B1B2 edge of $B_8H_8^{2-}$ (**1a**) (structure **4a**). The extra hydrogen in $B_8H_9^-$ destabilizes the structure with a tetragonal face and makes the boron skeleton slightly more rigid toward the DSD rearrangement. The observed $^{11}B$ NMR chemical shifts, the 2:4:2 intensity pattern, and the topomerization barrier assigned to a second $B_8H_8^{2-}$ form are all consistent with the computed values for **4a**. While no $B_8H_8^{2-}$ form is found to correspond with the 2:4:2 NMR chemical shift pattern, we raise the possibility that the second species observed under certain conditions might be the protonated form, $B_8H_9^-$ (**4a**), rather than a second $B_8H_8^{2-}$ isomer **1b**.

**Acknowledgment.** This work was supported by the Deutsche Forschungsgemeinschaft, the Fonds der Chemischen Industrie, the Stiftung Volkswagenwerk, and Convex Computer Corp. We thank Professor W. Kutzelnigg and Dr. M. Schindler for the Convex version of the IGLO program which is available for distribution, and R. E. Williams for helpful criticism and suggestions. M.B. acknowledges a grant of the Studienstiftung des Deutschen Volkes. The calculations were performed on a Cray Y-MP4 of the Leibniz Rechenzentrum Munich and on a Convex C-220s of the Institut für Organische Chemie.

**Registry No.** **1**, 12430-13-6; **4**, 122861-36-3.